Toxicology and Applied Pharmacology 236 (2009) 310–318

Contents lists available at ScienceDirect

Toxicology and Applied Pharmacology

journal homepage: www.elsevier.com/locate/ytaap

Interactions of silver nanoparticles with primary mouse fibroblasts and liver cells

S. Arora, J. Jain, J.M. Rajwade, K.M. Paknikar *

Centre for Nanobioscience, Agharkar Research Institute, G.G. Agarkar Road, Pune 411004, India

ARTICLE INFO

Article history:
Received 3 December 2008
Revised 18 February 2009
Accepted 24 February 2009
Available online 6 March 2009

Keywords:
Silver nanoparticles
Localization
Oxidative stress
Apoptosis
Primary fibroblasts
Primary liver cells

ABSTRACT

Primary cells are ideal for *in vitro* toxicity studies since they closely resemble tissue environment. Here, we report a detailed study on the *in vitro* interactions of 7–20 nm spherical silver nanoparticles (SNP) with primary fibroblasts and primary liver cells isolated from Swiss albino mice. The intended use of silver nanoparticles is in the form of a topical antimicrobial gel formulation for the treatment of burns and wounds.

Upon exposure to SNP for 24 h, morphology of primary fibroblasts and primary liver cells remained unaltered up to 25 μg/mL and 100 μg/mL SNP, respectively, although with minor decrease in confluence. IC_{50} values for primary fibroblasts and primary liver cells as revealed by XTT assay were 61 μg/mL and 449 μg/mL, respectively. Ultra-thin sections of primary cells exposed to 1/2 IC_{50} SNP for 24 h, visualized under Transmission electron microscope showed the presence of dark, electron dense, spherical aggregates inside the mitochondria, and cytoplasm, probably representing the intracellular SNP. When the cells were challenged with ~1/2 IC_{50} concentration of SNP (i.e. 30 μg/mL and 225 μg/mL for primary fibroblasts and primary liver cells, respectively), enhancement of GSH (~1.2 fold) and depletion of lipid peroxidation (~1.4 fold) were seen in primary fibroblasts which probably protect the cells from functional damage. In case of primary liver cells; increased levels of SOD (~1.4 fold) and GSH (~1.1 fold) as compared to unexposed cells were observed. Caspase-3 activity assay indicated that the SNP concentrations required for the onset of apoptosis were found to be much lower (3.12 μg/mL in primary fibroblasts, 12.5 μg/mL in primary liver cells) than the necrotic concentration (100 μg/mL in primary fibroblasts, 500 μg/mL in primary liver cells). These observations were confirmed by CLSM studies by exposure of cells to 1/2 IC_{50} SNP (resulting in apoptosis) and 2× IC_{50}) cells (resulting in necrosis).

These results clearly suggest that although silver nanoparticles seem to enter the eukaryotic cells, cellular antioxidant mechanisms protect the cells from possible oxidative damage. This property, in conjunction with the finding that primary cells possess much higher SNP tolerance than the concentration in the gel (~20 μg/g), indicates preliminary safety of the formulation and warrants further study for possible human application.

Introduction

Silver nanoparticles are emerging as one of the fastest growing product categories in the nanotechnology industry with focus on antimicrobial activity. This has led to increasing number of medical applications of silver nanoparticles. Some of the products which are already available in the market include wound dressings, contraceptive devices, surgical instruments and bone prostheses (Cheng et al., 2004; Chen et al., 2006; Cohen et al., 2007; Zhang et al., 2007; Lee et al., 2007). Apart from these applications, silver nanoparticles are being used for water purification, indoor air quality management (Cheng et al., 2004; Jain and Pradeep, 2005; Zhang and Sun, 2007). Thus, use of nanosilver is becoming more and more widespread in medicine and related applications. Such increasing exposure poses toxicological and environmental issues which need to be addressed (Chen and Schluesener, 2008).

As a part of an on-going program in our laboratory to develop a topical antimicrobial agent for the treatment of burn wound infections, silver nanoparticles (SNP) were prepared by a proprietary process and were demonstrated to possess broad spectrum antimicrobial activities at concentrations ranging between 0.78–6.12 μg/mL. The intended use of SNP is in the form of water soluble gel (prepared using a polymer like Carbopol®, containing 20 μg SNP per gram gel) for topical applications in treatment of burn wounds. For *in vitro* studies with SNP (intended for topical applications), the selection of cell types representing the target tissue is important. In the wound healing process, dermal fibroblasts are the main cell types implicated in extracellular matrix production (Hunt and Hopt, 1997). In earlier studies Takenaka et al. (2001) reported that liver appears to be a major accumulation site of circulatory silver nanoparticles. A recent clinical report also described absorption of nanosilver into the circulation following the use of nanosilver coated dressings for burns (Trop et al., 2006). Established cell lines are easy to maintain and are preferred in most toxicological studies for better reproducibility of data. The question whether the established cell lines are adequate

* Corresponding author. Fax: +91 20 25651542.
E-mail address: kpaknikar@gmail.com (K.M. Paknikar).

0041-008X/$ – see front matter © 2009 Elsevier Inc. All rights reserved.
doi:10.1016/j.taap.2009.02.020

target cells has often been raised with regard to clinical relevance of data derived from *in vitro* studies (Hanks, 1996). In such cases, primary cells isolated from target tissues are desirable for cytotoxicity testing to simulate the *in vivo* situation more closely. Further, primary cultured liver cells (rodent or human origin) also represent a useful tool for studying toxicity, drug metabolism and enzyme induction (Davila and Acosta, 1993; Zurlo and Arterburn, 1996).

Thus, bearing in mind the potential target organs, primary cells viz. primary mouse fibroblasts and primary mouse liver cells were selected for *in vitro* toxicity studies of SNP. An attempt was made to study intracellular localization of SNP and elucidate the biochemical changes in the intracellular milieu at 1/2 IC_{50} concentration of SNP. Another purpose of this study was to carry out detailed investigation on the type of cell death (apoptotic/necrosis) after exposure to SNP by performing caspase-3 activity and visualization by fluorescence microscopy and CLSM upon acridine orange/ethidium bromide (AO/EB) double staining.

Materials and methods

Silver nanoparticles (SNP). Silver nanoparticles used in the present study were synthesized by a novel process that involves photo-assisted reduction of Ag^+ to metallic nanoparticles and their biostabilization (World Patent application under PCT No. WO/2006/001033). They were used as colloidal aqueous suspension and were found to retain their stability in the culture media. The nanoparticles were spherical (>90% particles in the size range of 7–20 nm, as revealed by high resolution TEM) exhibiting characteristic surface plasmon peak at 436 nm. The data on particle size distribution measured by dynamic light scattering (Zetasizer, Malvern Instruments, UK) revealed the presence of particles in size range of 6.5 to 43.8 nm, with average size 16.6 nm.

Chemicals and glassware. The plastic ware and glassware used for cell culturing were obtained from Nunc (Myriad industries, San Diego, California). Caspase-3 assay kit (colorimetric), Dulbecco's modified Eagle's medium (DMEM), fetal bovine serum (FBS), L-glutamine, Penicillin and Streptomycin were procured from Sigma Chemical Company (St. Louis, MO). Cell proliferation kit (XTT) was procured from Roche diagnostics GmbH (Mannheim, Germany). Glutathione reductase was purchased from Fluka chemika/biochemika (Fluka Chemie AG, Switzerland). All other analytical grade chemicals for biochemical studies were obtained from Sigma Chemical Company (St. Louis, MO).

Isolation and culture of primary cells. All experiments were carried out with strict adherence to guidelines for minimizing distress in experimental animals. Swiss albino mice (1 day old) were euthanized by cervical dislocation and sterilized with 70% ethanol. For the isolation of dermal fibroblasts, the dorsal skin was removed and incubated for 4 h with 0.1% trypsin, 0.02% EDTA in phosphate buffered saline (PBS, 0.1 M, pH 7.4, supplemented with penicillin 200 U/mL and streptomycin 200 μg/mL) at 4 °C, followed by mechanical separation of epidermis from dermis. To isolate fibroblasts, the dermis was minced finely and incubated with 200 U/mL of collagenase I for 1 h at 37 °C. Small cell aggregates were separated from large tissue fragments by gravitation sedimentation for 10 min at room temperature. The supernatant was carefully removed, and cells were collected by centrifugation (for 5 min at 50×*g*) and were cultured in 25 cm^2 culture flasks containing 5 mL growth medium (Dulbecco's modified Eagle's medium supplemented with L-glutamine (4 mM), Penicillin (100 Units/mL), Streptomycin (100 μg/mL) and 10% (v/v) heat inactivated fetal bovine serum) for 48 h. The cells were then re-plated twice to deplete from the culture the residual keratinocytes that do not survive re-plating in 10% FBS-DMEM. The fibroblasts were checked for their spindle shaped morphology (passage one) and used for future experiments.

For the isolation of liver cells, the excised liver was minced with a scalpel, and tissue fragments were then incubated and agitated at 37 °C in three alternative cycles of a solution containing 1% EDTA in Earle's balanced salt solution without calcium and a solution containing 200 U/mL collagenase and 0.02 mg/mL soybean trypsin inhibitor in calcium-containing Earle's balanced salt solution. Cells were washed three times in growth medium and recovered by centrifugation (for 5 min at 50×*g*) after each wash. Freshly isolated liver cells were plated in 25 cm^2 culture flasks containing 5 mL growth medium. During subculture, cells were detached by trypsinization when they reached 80% confluency and split (1:3). Growth medium was changed every 3 days. All the experiments were carried out between passage nos. 1 to 3 for both the primary cell types.

Cell morphology by phase contrast microscopy. Cells were plated into a 35 mm tissue culture plate at a density of 2×10^5 cells (in 2 mL growth medium). After overnight growth, supernatants from the culture plates were aspirated out and fresh aliquots of growth medium containing SNP in desired concentrations (6.25–100 μg/mL for primary fibroblasts and 12.5–200 μg/mL for primary liver cells) were added. The silver concentration in the nanoparticle preparation was determined using atomic absorption spectrometry, (AAnalyst800, Perkin Elmer, USA). Upon incubation, cells were washed with phosphate buffered saline (0.1 M PBS, pH 7.4) and the morphological changes were observed under an inverted phase contrast microscope at 200× magnification.

Cell viability assay. Cell viability was tested using XTT (Sodium 3′-[1-(phenylaminocarbonyl)-3,4-tetrazolium]-*bis* (4-methoxy-6-nitro) benzene sulfonic acid hydrate) assay (Gerlier and Thomasset, 1986) based on the cleavage of yellow tetrazolium salt XTT by metabolically active cells to form an orange formazan dye which was quantified

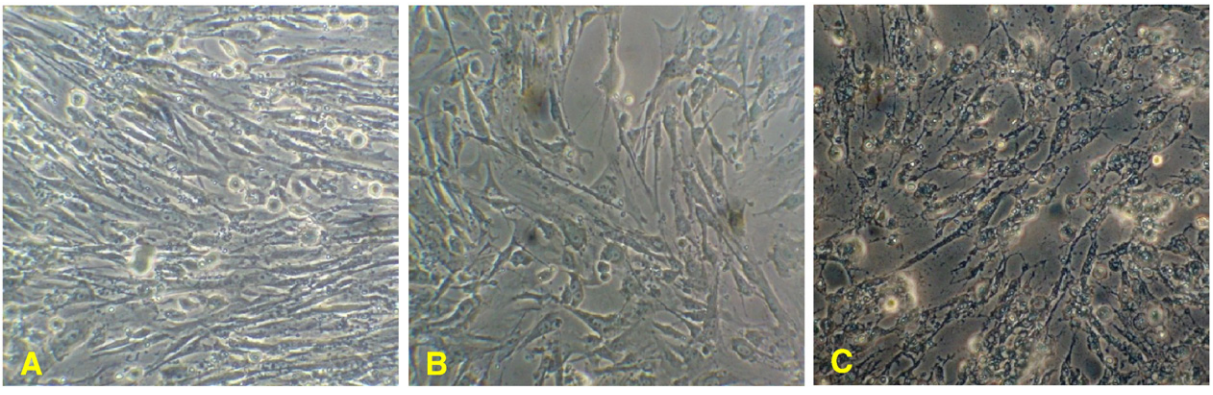

Fig. 1. Phase-contrast micrographs of primary fibroblasts: (A) unexposed cells; (B–C) 24 h after the cultures were exposed to 6.25 μg/mL and 100 μg/mL SNP, respectively (magnification×200).

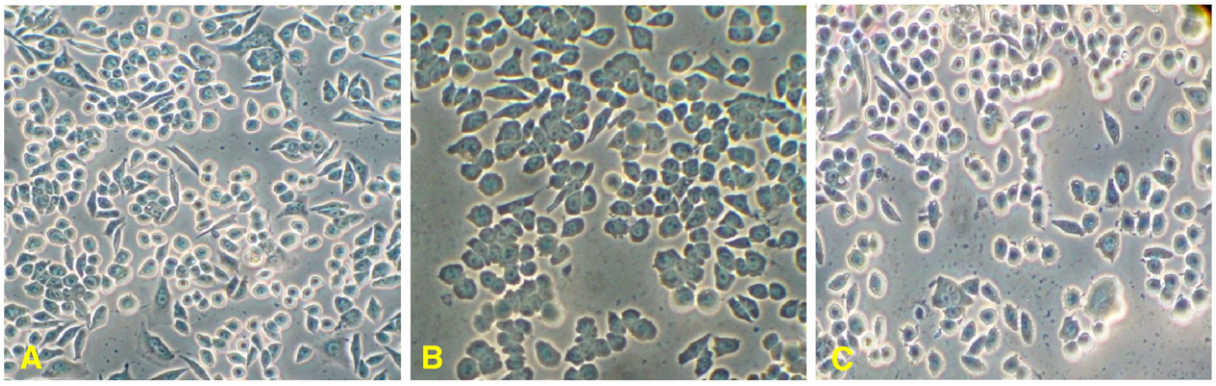

Fig. 2. Phase-contrast micrographs of primary liver cells: (A) unexposed cells; (B–F) 24 h after the cultures were exposed to 12.5 μg/mL and 200 μg/mL SNP respectively (magnification × 200).

using ELISA reader (Biorad, model no.680). XTT assay was performed according to the manufacturer's instructions with appropriate controls. Cells were seeded in 96 well microtitre plates (1×10^4 cells/200 μL growth medium/well) followed by overnight incubation. Supernatants from the wells were aspirated out and fresh aliquots of growth medium (containing SNP in desired concentrations in the range of 1.56–500 μg/mL) were added. After 24 h, supernatants were aspirated out and the cell monolayers in the wells were washed with 200 μL PBS (0.1 M, pH 7.4). Subsequently, XTT reagent (70 μL) was added in each well, incubated for 5 h and absorbance at two wavelengths (415 nm for soluble dye and 630 nm for cells) were recorded using ELISA reader. Concentrations of SNP showing 50% reduction in cell viability (i.e. IC_{50} values) were then calculated.

Transmission electron microscopy. Cells were plated into a 35 mm tissue culture plate at a density of 2×10^5 cells (in 2 mL growth medium). After overnight growth, supernatants from the culture plates were aspirated out and fresh aliquots of growth medium containing ~1/2 IC_{50} SNP were added. For control experiments, medium without nanoparticles was used. Upon incubation for 24 h, the cells (about 80% confluent) were trypsinized and recovered by centrifugation at 500×*g* for 5 min. Cell pellets were washed with phosphate buffer (0.1 M, pH 7.4). Cell pellets were fixed using 4% paraformaldehyde and 2.5% glutaraldehyde in 0.1 M phosphate buffer (pH 7.4) for 2 h followed by post-fixation in 1% osmium tetroxide (Agar Scientific, Stansted Essex, England, UK), for 1.5 h. Cell pellets were dehydrated through a series of ethanol concentrations (20%, 30%, 40%, 50%, 60%, 70%, and 90%) followed by treatment with 2% uranyl acetate in 95% ethanol (Enblock stain) for 1 h and further dehydration with 100% ethanol for 1 h. Cell pellets were finally treated with propylene oxide (twice for 15 min each) followed by 1:1 propylene oxide:araldite resin overnight. Cell pellets were infiltrated with fresh araldite resin (3 changes with a gap of 3 to 4 h). Cell pellets were subsequently embedded in araldite resin at 60 °C for 48 h and ultra-thin sections (70 nm–80 nm) were cut with glass knives in an ultra microtome (LEICA EM UC6, Netherlands). The sections were mounted on copper grids and stained with 1% aqueous uranyl acetate and 0.2% lead citrate (Reynolds, 1963). The stained sections were scanned with an electron microscope (TECHNAI G2 SPIRIT BIOTWIN, Netherlands) for ultra structural observations at 80 kV.

Preparation of cell extract and biochemical assays. For the preparation of cell extract, 75 cm^2 flasks containing 15 mL of growth medium were seeded with ca. 1×10^7 cells as described by Christopher et al. (2004). After overnight growth the cells were challenged with ~1/2 IC_{50} SNP (viz., 30 μg/mL and 225 μg/mL for primary fibroblasts and primary liver cells respectively) and incubated for 24 h. The cells (about 80% confluent) were then trypsinized and pelleted by centrifugation at 500×*g* for 5 min. The cell pellet was washed with PBS (0.1 M, pH 7.4), resuspended in 500 μL chilled homogenizing buffer (250 mM Sucrose, 12 mM Tris–HCl, 0.1 mM DTT, pH 7.4) and lysed using Dounce homogenizer. The lysate was centrifuged (8000×*g*, 10 min, 4 °C) and the supernatant (cell extract) was used

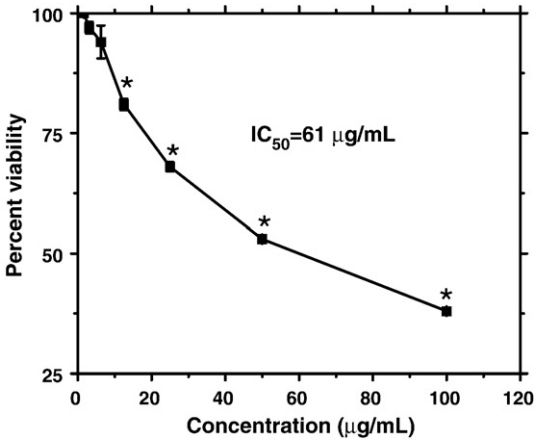

Fig. 3. Percent viability measured by XTT assay on primary fibroblasts after treatment with SNP (1.56 μg/mL to 100 μg/mL) for 24 h. The data are expressed as mean ± standard deviation (SD) of three independent experiments. An OD value of control cells (unexposed cells) was taken as 100% viability (0% cytotoxicity). Asterisk (*) denotes a statistically significant difference compared to control ($p<0.05$).

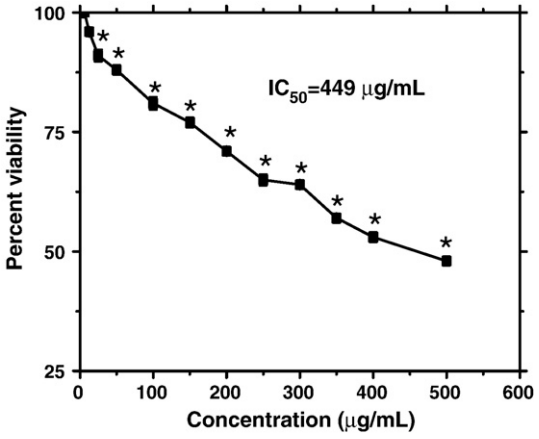

Fig. 4. Percent viability measured by XTT assay on primary liver cells after treatment with SNP (1.56 μg/mL to 500 μg/mL) for 24 h. The data are expressed as mean ± standard deviation (SD) of three independent experiments. An OD value of control cells (unexposed cells) was taken as 100% viability (0% cytotoxicity). Asterisk (*) denotes a statistically significant difference compared to control ($p<0.05$).

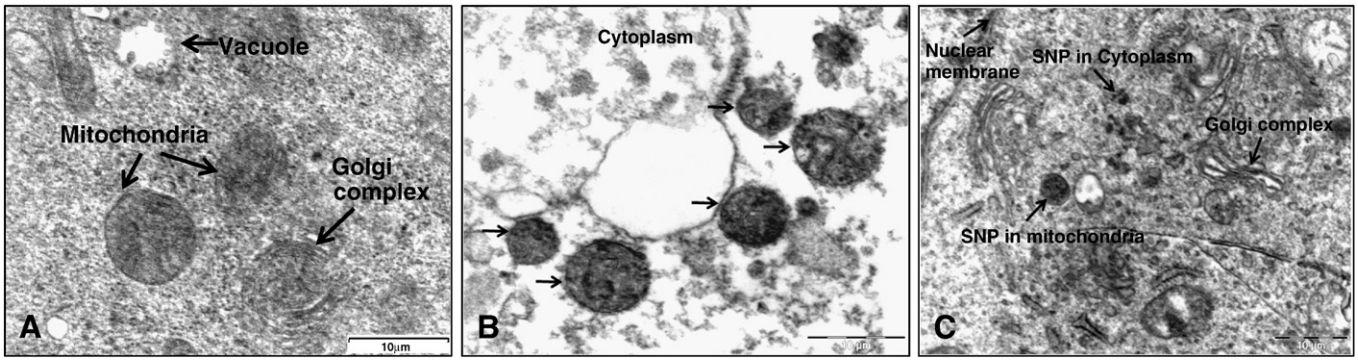

Fig. 5. (A) Transmission electron micrographs of unexposed (control) cells, arrows showing the cellular structures viz. mitochondria, golgi complex, vacuole and cytoplasm. (B) Transmission electron micrographs of primary fibroblasts after the cultures were exposed to ~1/2 IC_{50} SNP (30 μg/mL) for 24 h, arrows showing the presence of SNP in the mitochondria. (C) Transmission electron micrographs of primary liver cells after the cultures were exposed to ~1/2 IC_{50} SNP (225 μg/mL) for 24 h, showing the presence of SNP in the cytoplasm and mitochondria. (Scale marker indicates 10 μm.)

in various biochemical assays. Protein concentration in the cell extract was estimated by Bradford (1976) method.

Superoxide dismutase. Superoxide dismutase activity was measured according to the method described by Kono (1978). Briefly, the reaction mixture (2.1 mL) contained 1924 μL sodium carbonate buffer (50 mM), 30 μL nitrobluetetrazolium (1.6 mM), 6 μL Triton X-100 (10%) and 20 μL hydroxylamine–HCl (100 mM). Subsequently 100 μL cell extract was added and absorbance (560 nm) was read for 5 min against blank (reaction mixture sans cell extract). Change in absorbance per min (i.e. ΔA_{560}) was calculated and used in the estimation of enzyme activity (extinction coefficient value used was 9920 M^{-1} cm^{-1}).

Total glutathione (reduced) content. Total GSH content was measured as described by Saldak and Lindsay (1968). The reaction mixture containing 1.2 mL EDTA (0.02 M), 1 mL distilled water, 250 μL 50% trichloroacetic acid, 50 μL Tris buffer (0.4 M, pH 8.9) was centrifuged at 300×*g* for 15 min. Clear supernatant (500 μL) was mixed with 1 mL of 0.4 M Tris buffer (containing 0.02 M EDTA, pH 8.9), 100 μL of 0.01 M DTNB [5,5′-dithio-*bis*-(2-nitrobenzoic acid)] and 100 μL cell extract. The mixture was incubated at 37 °C for 25 min and the yellow color developing was read at 412 nm against blank. The enzyme activity was calculated taking the extinction coefficient as 14150 M^{-1} cm^{-1}.

Lipid peroxidation. In this method described by Beuge and Aust (1978), a mixture of 100 μL Tris buffer (150 mM, pH = 7.1), 10 μL ferrous sulfate (100 mM), 10 μL ascorbic acid (150 mM), 780 μL distilled water and 100 μL cell extract was incubated at 37 °C for 15 min. Thiobarbituric acid (0.375%, 2 mL) was then added to the mixture and allowed to react at 100 °C (in water bath) for 15 min. The reaction mixture was then centrifuged (800×*g* for 10 min) and supernatant was read at 532 nm against blank. The enzyme activity was calculated (extinction coefficient value used was 156,000 M^{-1} cm^{-1}).

Apoptotic assays. Caspase-3 colorimetric assays were performed using a standard kit (Sigma, USA) to determine the concentrations of SNP inducing apoptosis and necrosis in cells. Further, to visualize apoptotic/necrotic nuclei, cells were seeded on glass coverslips (18×18 mm) placed into 35 mm tissue culture plates at a density of

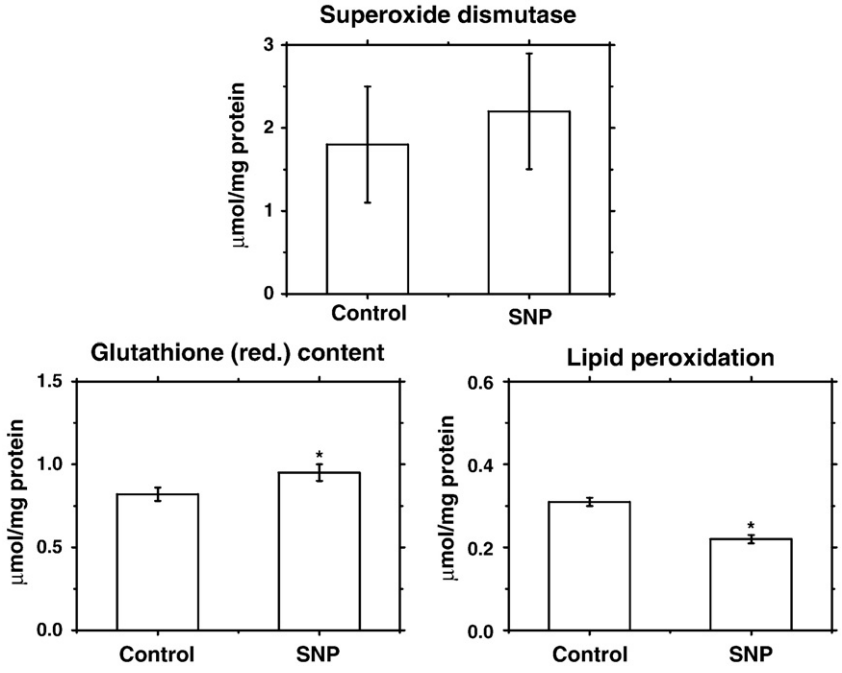

Fig. 6. Levels of SOD, GSH and lipid peroxidation in untreated (control) and treated (with ~1/2 IC_{50} SNP, 30 μg/mL for 24 h) primary fibroblasts. The data are expressed as mean ± standard deviation (SD) of three independent experiments. Asterisk (*) denotes a statistically significant difference compared to control ($p<0.05$).

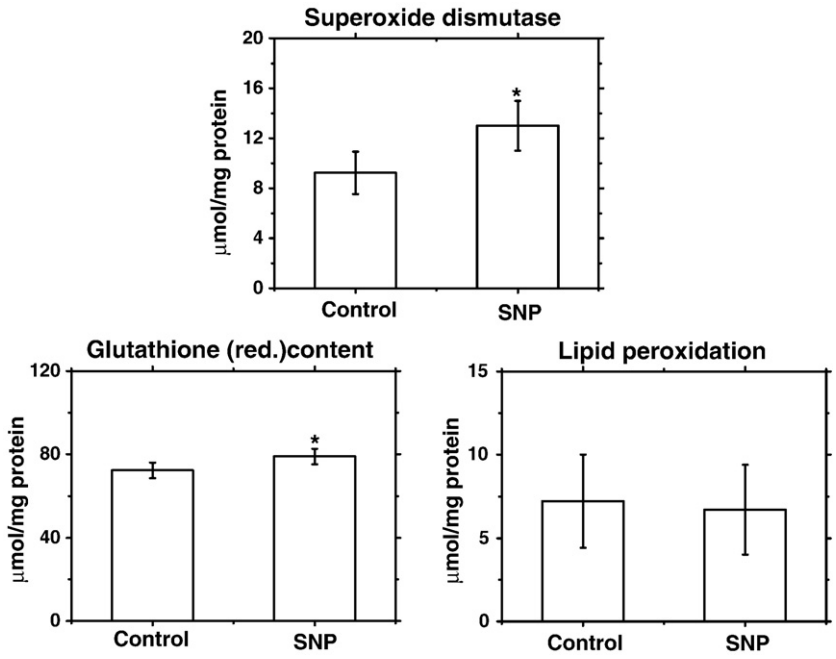

Fig. 7. Levels of SOD, GSH and lipid peroxidation in untreated (control) and treated primary liver cells (with ~1/2 IC_{50} SNP, 225 μg/mL for 24 h). The data are expressed as mean ± standard deviation (SD) of three independent experiments. Asterisk (*) denotes a statistically significant difference compared to control ($p<0.05$).

2×10^5 cells (in 2 mL growth medium). After overnight growth, supernatants from the culture plates were aspirated out and fresh aliquots of growth medium containing SNP at desired concentrations (~1/2 IC_{50} and ~2× IC_{50}) were added. Upon incubation for 24 h, cells were washed with PBS and fixed in 4% chilled paraformaldehyde for 20 min and then washed twice with PBS. Cells were stained by adding 1 mL AO/EB mix (100 μg/mL AO and 100 μg/mL EB in PBS). After 2 min incubation, cells were washed twice with PBS (5 min each) and visualized under a fluorescence microscope (Zeiss Axio star plus, USA) at 400× magnification with excitation filter 480/30 nm. Three independent cell counts (counting a minimum of 100 total cells each) were obtained on the basis of differential staining of the nuclei (live cells have a normal green nucleus; early apoptotic cells have bright green nucleus with condensed or fragmented chromatin; late apoptotic cells display condensed and fragmented orange chromatin; necrotic cells display a structurally normal orange nucleus). These results were supported by confocal laser scanning microscopy (CLSM). For this cells were mounted with anti-fade mounting medium (Chemicon, USA) and observed (at 400× magnification) under confocal laser scanning microscope (CLSM 510, version 2.01; Zeiss, USA) after excitation at 488 nm. Green fluorescence was detected with a band pass filter ranging between 505 and 530 nm. Simultaneously, red fluorescence was detected using the long pass filter at 585 nm, and superimposition of both green and red fluorescence generated the final images.

Statistical analyses. All the experiments were carried out three times, independently. The data obtained were expressed in terms of 'mean ± standard deviation' values. Wherever appropriate, the data were also subjected to unpaired two tailed Student's *t*-test. A value of $p<0.05$ was considered as significant.

Results

Under phase contrast microscope, primary fibroblasts (control) appeared polyhedric or stellate showing slender lamellar expansions (Fig. 1A) that joined neighboring cells. No changes in the cellular

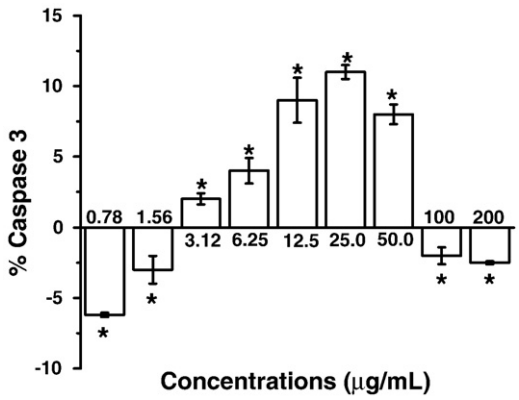

Fig. 8. Caspase-3 activity assay for primary fibroblasts. SNP induce caspase-3 production (apoptosis) at concentrations in the range of 3.12–50 μg/mL. At SNP concentrations ≥100 μg/mL, caspase-3 activity was not detected indicating necrosis. An OD value of positive control was taken as 100%. Asterisk (*) denotes a statistically significant difference compared to control ($p<0.05$).

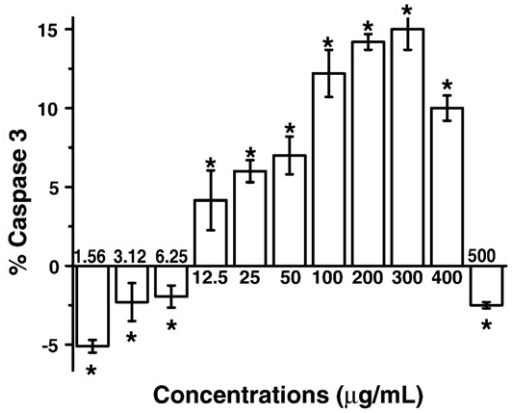

Fig. 9. Caspase-3 activity assay for primary liver cells. SNP induce caspase-3 production (apoptosis) at concentrations in the range of 12.5–400 μg/mL. At SNP concentrations ≥500 μg/mL, caspase-3 activity was not detected indicating necrosis. An OD value of positive control was taken as 100%. Asterisk (*) denotes a statistically significant difference compared to control ($p<0.05$).

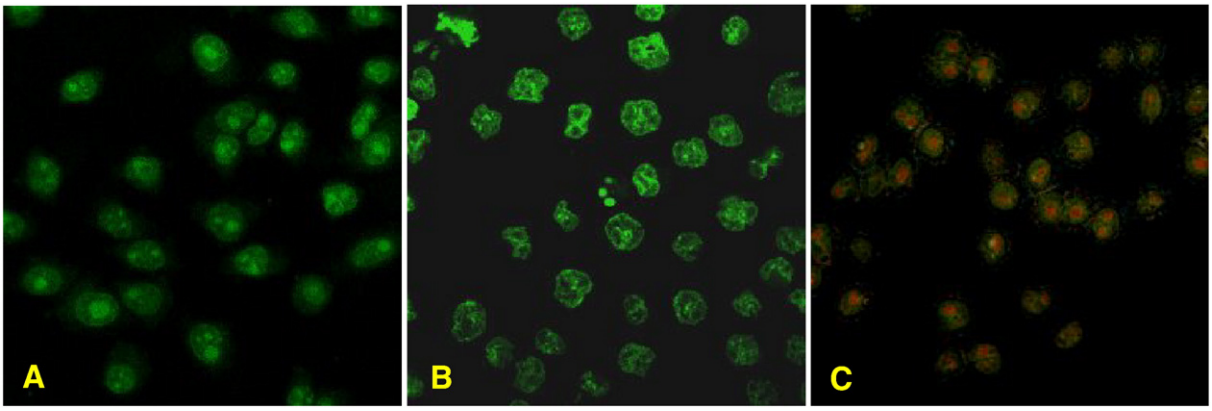

Fig. 10. Confocal micrographs (magnification × 400) of AO/EB stained primary fibroblasts. (A) Unexposed (control) cells have a normal green nucleus indicating live cells. (B) Cells exposed to ~ 1/2 IC_{50} SNP (30 μg/mL) for 24 h display bright green nucleus with condensed or fragmented chromatin suggesting apoptosis. (C) Cells exposed to ~ 2× IC_{50} SNP (120 μg/mL) for 24 h have a structurally normal orange nucleus indicative of necrosis.

morphology were observed upto 25 μg/mL SNP. With increasing concentration of SNP (from 50 μg/mL to 100 μg/mL), cells were observed to be less polyhedric, more fusiform, and shrunken. Representative micrographs (Figs. 1B and C) have been shown. Primary liver cells occurred as single cells and viable cells were flattened (control) varying from wedge-shaped to hexagonal in shape (Fig. 2A). SNP (12.5–100 μg/mL) treated primary liver cells showed no morphological changes compared to control cells. Primary liver cells appeared refractive with damaged irregular cell membranes at concentrations ≥200 μg/mL SNP. Representative micrographs (Figs. 2B and C) have been shown.

The results of XTT assays showed a dose-dependent decrease in viability for both the cell types with IC_{50} values working out as 61 μg/mL and 449 μg/mL for primary fibroblasts (Fig. 3) and primary liver cells (Fig. 4), respectively.

Transmission electron microscopic studies revealed that dark, electron dense, spherical aggregates were found inside the mitochondria of exposed primary fibroblasts (Fig. 5B) and mitochondria and vacuoles of primary liver cells (Fig. 5C) as compared to unexposed (control) cells (Fig. 5A). These electron dense regions represent the intracellular silver nanoparticles.

When antioxidant defense mechanisms were investigated, biochemical changes occurring in the SNP treated cells were monitored (with respect to enzyme activity indicative of oxidative stress), interesting data emerged. In primary fibroblasts (Fig. 6), treatment with SNP decreased lipid peroxidation by ~1.4 folds (0.31 μmol/mg protein in unexposed cells and 0.22 μmol/mg protein in SNP-exposed cells). In contradistinction, there was ~1.2 fold increase in GSH levels after SNP treatment (0.95 μmol/mg protein as compared to 0.82 μmol/mg protein in control cells). Changes observed in the levels of SOD were not statistically significant.

In case of primary liver cells (Fig. 7) levels of GSH increased ~1.1 folds after treatment with SNP (79 μmol/mg protein as compared to 72.3 μmol/mg protein in control cells). SOD levels were found to be ~1.4 fold higher in SNP treated cells (13 μmol/mg protein) as compared to unexposed cells (9.2 μmol/mg protein). Changes in the levels of lipid peroxidation in primary liver cells were statistically insignificant.

In both the primary cell types, the apoptotic thresholds of SNP were monitored by caspase-3 assay after exposure to SNP for a range of doses (0.78–500 μg/mL). The results of a representative dose-range study are shown in Figs. 9 and 10. In case of primary fibroblasts (Fig. 8), SNP could induce apoptosis at concentrations in the range of 3.12–50 μg/mL. For primary liver cells (Fig. 9) this range changed to 12.5–400 μg/mL. In case of primary fibroblasts, under CLSM, normal green nucleus was observed in control cells (Fig. 10A). Exposure to 30 μg/mL (~ 1/2 IC_{50}) SNP resulted in apoptosis (bright green nucleus with condensed or fragmented chromatin) of cells (Fig. 10B). Further, at SNP concentration 120 μg/mL (~2× IC_{50}) cells with structurally normal but orange stained nuclei were observed (Fig. 10C) suggesting necrosis. Primary liver cells unexposed to SNP (control cells) show normal green nucleus (Fig. 11A), whereas cells exposed to 1/2 IC_{50} SNP (225 μg/mL) display bright green nuclei with condensed or fragmented chromatin (Fig. 11B) which indicates apoptosis. Liver cells with structurally normal orange nuclei (Fig. 11C) were observed at

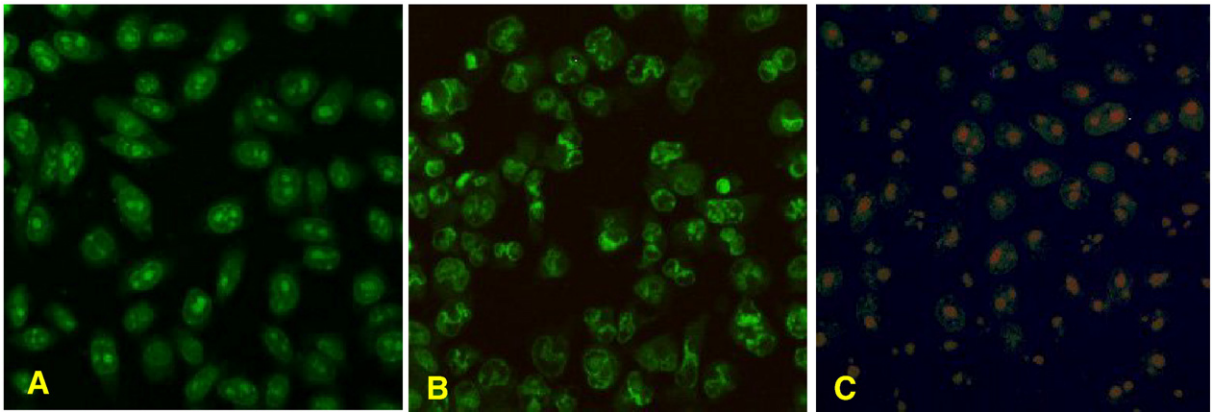

Fig. 11. Confocal micrographs (magnification × 400) of AO/EB stained primary liver cells. (A) Unexposed (control) cells have a normal green nucleus indicating live cells. (B) Cells exposed to ~ 1/2 IC_{50} SNP (225 μg/mL) for 24 h display bright green nucleus with condensed or fragmented chromatin suggesting apoptosis. (C) Cells exposed to ~2× IC_{50} SNP (900 μg/mL) for 24 h have a structurally normal orange nucleus indicative of necrosis.

Table 1
Quantification of AO/EB stained primary fibroblasts after exposure to SNP (~1/2 IC_{50} SNP and 2× IC_{50}) for 24 h as compared to unexposed cells using under fluorescence microscope (magnification × 200).

Primary fibroblasts (%)			
Type of cells	Control (unexposed) cells	Exposed to ~1/2 IC_{50} SNP (30 μg/mL)	Exposed to ~2× IC_{50} SNP (120 μg/mL)
Live cells	96 ± 2	69 ± 2*	37 ± 1*
Apoptotic cells	3 ± 1	24 ± 2*	17 ± 2*
Necrotic cells	1 ± 1	7 ± 3	46 ± 3*

The data are expressed as mean ± standard deviation (SD) of three independent experiments. Asterisk (*) denotes a statistically significant difference compared to control ($p<0.05$).

SNP concentration ~2× IC_{50} (900 μg/mL) indicating necrosis. Table 1 and Table 2 show quantitative data on the percentage of live, apoptotic and necrotic cells after exposure to ~1/2 IC_{50} and ~2× IC_{50} SNP as compared to control cells. For primary fibroblasts (Table 1), 69% live cells, 24% apoptotic cells and 7% necrotic cells were observed at SNP concentration 30 μg/mL (~1/2 IC_{50}) whereas, at 4 folds higher SNP concentration (~2× IC_{50}), live as well as apoptotic cell population decreased by 1.8 folds and 1.4 folds respectively, whereas, an increase in the necrotic cell population (6.5 folds) was noticed. In case of primary liver cells (Table 2) the live cell population and apoptotic cell population decreased 2.2 folds and 1.7 folds respectively; necrotic cell population increased 11 folds at ~2× IC_{50} SNP i.e. 900 μg/mL as compared to ~1/2 IC_{50} (225 μg/mL).

Discussion

In the present work we have attempted a detailed investigation on the effects of silver nanoparticles (SNP) in primary cells. Even though nanosilver-based wound dressings have received approval for clinical applications their possible dermal toxicity is reported to be a matter of concern (Chen and Schluesener, 2008). The intended use of these SNP is in the form of water soluble gel formulation (prepared using a polymer such as Carbopol®) for treatment of wounds in the form of a topical formulation. The earlier studies on toxicity of silver nanoparticles have dealt with chemically synthesized silver nanoparticles and dressings (carboxymethylcellulose, polyethylene mesh, charcoal dressing, polymeric fabric etc.) impregnated with nanosized silver with special applications for treatment of wound infections (Bhattacharya and Mukherjee, 2008). Nanocrystalline silver containing gel formulation is in fact, the first product of its kind for topical applications which was being developed in our laboratory and therefore was a 'non-generic' or a 'new material' requiring detailed studies on toxicological aspects. After reviewing the literature a fact is noticeable that for the limited number of cell lines tested (C18-4 germ cell line, BRL 3A liver cell line and PC-12 neuroendocrine cell line) exposure to silver nanoparticles significantly decreased the function of mitochondria. Apoptosis or apoptosis-like change of cell morphology also occurred in all three cell lines following exposure (Braydich-Stolle et al., 2005; Hussain et al., 2005, 2006) to silver nanoparticles. In our previous study, we have also demonstrated similar effects on HT-1080 and A-431 cell lines (Arora et al., 2008). There are very few studies documented in literature which elucidate the intracellular localization of silver nanoparticles (Chung et al., 2008). Apart from this, when genotoxic effects and cell death are studied, more than two independent assays are not performed. Regarding the mode of cell death, a combination of at least three criteria of cell death should be evaluated to draw the correct conclusions (Morgan, 2005). Studies that quantify the effects of silver nanoparticles on primary cells are scarce even though they are a true representative of tissue and hence are ideal for *in vitro* toxicity studies. *In vitro* methods are being used extensively as adjuncts to complement investigations conducted *in vivo* as part of hierarchical testing strategy. Thus *in vitro* systems contribute to genuine reduction in number of *in vivo* experiments conducted. A major promise of *in vitro* systems is to obtain mechanism derived information that is considered pivotal for adequate risk assessment. Primary screening *in vivo* is always justified to permit oral administration and adequate bioavailability (Straughan et al., 1997). Since SNP based gel formulation is aimed at topical application, *in vitro* data could be extrapolated to *in vivo*, thus minimizing experimentation in living animals.

The toxicity of SNP was evaluated by studying cellular morphology and mitochondrial function (XTT assay) under control and exposed conditions. At this stage, we did not know whether these SNP are interacting with cells physically from outside or going inside the cells. To answer this question, localization studies were carried out by Transmission Electron Microscopy (TEM) after exposing the cells to SNP. To investigate the potential role of oxidative stress as a mechanism of SNP induced toxicity, the effects on SOD, GSH and lipid peroxidation were monitored. It is now well established that the generation or external addition of ROS can cause cell death by two distinct cell death pathways, viz. apoptosis or necrosis. Necrosis is detrimental for wound healing and often results in healing with scar formation (Tian et al., 2007). ROS are known to activate caspases, which are considered as the executioners of apoptosis (Cohen, 1997; Fadeel et al., 1998). Gopinath et al. (2008) have also shown involvement of caspase in silver nanoparticles mediated apoptosis in the baby hamster kidney (BHK21) and human colon adenocarcinoma (HT29) cell lines. The correlation between oxidative stress and apoptosis, as explained above prompted us to investigate the type of cell death in SNP toxicity. Fluorescence light microscopy with differential uptake of fluorescent DNA binding dyes (AO/EB staining) is a method of choice (for its simplicity, rapidity, and accuracy) that distinguishes between apoptotic and necrotic cell populations. Acridine orange (AO) permeates all cells and makes the nuclei appears green. Ethidium bromide (EB) is only taken up by cells when cytoplasmic membrane integrity is lost, and stains the nucleus red. EB also dominates over AO. Thus live cells have a normal green nucleus; early apoptotic cells have bright green nucleus with condensed or fragmented chromatin; late apoptotic cells display condensed and fragmented orange chromatin; cells that have died from direct necrosis have a structurally normal orange nucleus (Renvoize et al., 1998). To support these findings, typical apoptotic or necrotic features in cells were also observed under CLSM.

Results obtained by us clearly showed that cell morphology of primary fibroblasts and primary liver cells was unaltered in the presence of SNP up to a concentration of 25 μg/mL and 100 μg/mL, respectively which is an indication of safety of SNP up to these concentrations. The effect of SNP on cell viability could be quantified using XTT assay as the amount of XTT reduced per unit time is proportional to the cell number (Harbell et al., 1997). Decreased mitochondrial function in cells exposed to SNP (1.56–500 μg/mL) in a dose-dependent manner was evident in the XTT assay. The IC_{50} values of SNP were found to be 61 μg/mL and 449 μg/mL for primary fibroblasts and primary liver cells, respectively which is much higher than the

Table 2
Quantification of AO/EB stained primary liver cells after exposure to SNP (~1/2 IC_{50} SNP and 2× IC_{50}) for 24 h as compared to unexposed cells using under fluorescence microscope (magnification × 200).

Primary liver cells (%)			
Type of cells	Control (unexposed) cells	Exposed to ~1/2 IC_{50} SNP (225 μg/mL)	Exposed to ~2× IC_{50} SNP (900 μg/mL)
Live cells	98 ± 1	71 ± 3*	32 ± 2*
Apoptotic cells	2 ± 1	24 ± 2*	14 ± 1*
Necrotic cells	0	5 ± 2	54 ± 1*

The data are expressed as mean ± standard deviation (SD) of three independent experiments. Asterisk (*) denotes a statistically significant difference compared to control ($p<0.05$).

secondary cells (viz. 10.6 μg/mL and 11.6 μg/mL for HT1080 and A431 cells, respectively) as observed in our previous study (Arora et al., 2008). This suggests that the primary cells are more resistive to SNP treatment as compared to secondary cell lines and primary liver cells are inherently more resistant to SNP treatment as compared to primary fibroblasts. Similar observations were reported by Moller et al. (2002) where cell viability was shown to be higher for primary alveolar macrophages, as compared to J774A.1 (reticulum cell sarcoma) cell line after exposure to 100 μg/mL ultrafine test particles (UFP) per mL for 24 h.

Ultra-thin sections of established cells as well as primary cells exposed to ~1/2 IC_{50} SNP for 24 h, visualized under Transmission electron microscope showed the presence of dark, electron dense, spherical aggregates inside various cellular structures such as the mitochondria, and cytoplasm. These structures could probably represent the intracellular SNP. Lopotko et al. (2007) have also demonstrated that interaction of nanoparticles with cells leads to the formation of nanoparticles clusters (NPCs) in various cellular organelles viz., endosomes and vacuoles via endocytosis.

Mitochondria represent the most active cellular redox organelles and localization of these particles into such redox active centers is expected to cause alterations in various antioxidant enzyme systems that are functional here. Thus as it happens, in case of nanoparticles of various chemistries, particles are taken up into cells via endocytic pathways and get localized mainly to mitochondria (Foley et al., 2002; Li et al., 2003). The presence of SNP inside the mitochondria could lead to alterations in ROS production, thereby interfering with cellular antioxidant defenses. Therefore in the present study, an attempt was made to elucidate the biochemical changes in the cells at ~1/2 IC_{50} (i.e. 30 μg/mL and 225 μg/mL for primary fibroblasts and primary liver cells, respectively) concentration of SNP. Here the most critical issue to be addressed was the concentration of SNP. Concentrations ≥IC_{50} were deliberately not chosen as these would result in a population of cells with at least 50% cells in the death phase. Hence, a concentration of SNP (~1/2 IC_{50}) was selected to maintain uniformity for comparison between two or more cell types and the concentration ensured >90% cell viability. Another argument is that at concentrations ~1/2 IC_{50} certain biochemical changes at the cellular level could have occurred even though apparent cell damage or death was not observed. This would provide biochemical evidence to the mechanisms underlying the interactions of SNP with eukaryotic cells. The results obtained, i.e. enhancement of GSH (~1.2 fold) and depletion of lipid peroxidation (~1.4 fold) indicated that primary fibroblasts were protected from functional damage. In case of primary liver cells; increased levels of SOD (~1.4 fold) and GSH (~1.1 fold) as compared to unexposed cells were observed. These results suggest that oxidative stress induced to cells after exposure to SNP was sufficient to trigger antioxidant defense mechanisms.

On the whole, data obtained by us clearly suggest that oxidative stress does not persist long enough to cause oxidative damage in case of SNP exposed primary cells, at ~1/2 IC_{50} concentrations. The oxidative stress is taken care of by antioxidant enzyme system of primary cells.

It is well known that oxidative stress can lead to cell death; either by apoptosis or necrosis. Severe oxidative stress to cells causes necrosis and moderate oxidative stress causes apoptosis (Curtin et al., 2002). In wound healing, ideally cell death should not occur; but if at all it occurs, the apoptotic cell death is preferred over necrotic cell death (Tian et al., 2007). Absence of inflammation during apoptosis favors scar less wound healing. Hence studies on type of cell death were carried out. To make the right interpretation of data and to draw the correct conclusions regarding the mode of cell death after exposure to SNP, it is recommended that a combination of at least three criteria of cell death be evaluated: cell morphology, DNA fragmentation, annexin V binding, and/or caspase activation (Morgan, 2005). In the present study the type of cell death (apoptosis/necrosis) after SNP exposure was evaluated by DNA laddering, caspase-3 activity assays and visualization by fluorescence microscopy and CLSM upon acridine orange /ethidium bromide (AO/EB) double staining. Caspase-3 activity assay data clearly show that at concentrations up to 100 μg/mL and 500 μg/mL (for primary fibroblasts and primary liver cells, respectively) cell death occurs due to apoptosis alone. Cytotoxicity (necrosis) at higher doses of SNP (≥100 μg/mL for primary fibroblasts and ≥500 μg/mL for primary liver cells) could be clearly demonstrated by total lack of caspase-3 activity. These results were further corroborated by fluorescence microscopy and CLSM studies after AO/EB double staining. For both the primary cell types, apoptotic cell population decreased with a concomitant increase in the necrotic cell population at ~2× IC_{50} SNP in contradistinction to ~1/2 IC_{50} (where apoptotic cell population was several folds higher than necrotic cells). These finding assumes considerable significance in clinical applications such as treatment of wounds where SNP could promote wound repair. Higher doses of SNP would however, elicit an inflammatory response (necrosis) which could adversely affect the wound healing process (Tian et al., 2007). Similar studies were done by Gopinath et al. (2008) on the baby hamster kidney (BHK21) and human colon adenocarcinoma (HT29) cell lines where necrosis starts at silver nanoparticles concentrations >44.0 μg/mL.

In summary, our studies show that although silver nanoparticles seem to enter the primary cells and cause oxidative stress, the cellular antioxidant mechanisms avert oxidative damage. The intended use of silver nanoparticles is in the form of a topical antimicrobial gel formulation for the treatment of burns and wounds. Our data show that primary cells possess much higher SNP tolerance than the concentrations encountered in the gel formulation (~20 μg/g). This preliminary indication of safety warrants further *in vivo* studies in animals, as the next step towards possible human application.

Conflict of interest statement

The authors declare that there are no conflicts of interest.

Acknowledgments

The authors are thankful to the Nano Cutting Edge Technology Pvt. Ltd., Mumbai for financial assistance, Interactive Research School for Health Affairs (IRSHA), Pune for providing animal tissue culture facility and National Center for Cell Sciences (NCCS), Pune for confocal laser scanning microscopy (CLSM). SA thanks CSIR, New Delhi for research fellowship.

References

Arora, S., Jain, J., Rajwade, J.M., Paknikar, K.M., 2008. Cellular responses induced by silver nanoparticles: *in vitro* studies. Toxicol. Lett. 179, 93–100.

Beuge, J.A., Aust, A.D., 1978. Microsomal lipid peroxidation. Methods Enzymol. 52, 302–310.

Bhattacharya, R., Mukherjee, P., 2008. Biological properties of "naked" metal nanoparticles. Adv. Drug Deliv. Rev. 60, 1289–1306.

Bradford, M., 1976. A rapid and sensitive method for the quantification of microgram quantities of protein utilizing the principle of protein-dye binding. Anal. Biochem. 72, 248–254.

Braydich-Stolle, L., Hussain, S., Schlager, J.J., Hofmann, M.C., 2005. *In vitro* cytotoxicity of nanoparticles in mammalian germ line stem cells. Toxicol. Sci. 88, 412–419.

Chen, X., Schluesener, H.J., 2008. Nanosilver: a nanoproduct in medical application. Toxicol. Lett. 176, 1–12.

Chen, J., Han, C.M., Lin, X.W., Tang, Z.J., Su, S.J., 2006. Effect of silver nanoparticle dressing on second degree burn wound. Zhonghua WaiKe ZaZhi 44, 50–52.

Cheng, D., Yang, J., Zhao, Y., 2004. Antibacterial materials of silver nanoparticles application in medical appliances and appliances for daily use. Chin. Med. Equip. J. 4, 26–32.

Christopher, O.I., Veera, L.B., Lambert, T.A., Lekan, M.L., John, W., 2004. Response of antioxidant enzymes and redox metabolites to cadmium-induced oxidative stress in CRL-1439 normal rat liver cells. Int. J. Mol. Med. 14, 87–92.

Chung, Y.C., Chen, I.H., Chen, C.J., 2008. The surface modification of silver nanoparticles by phosphoryl disulfides for improved biocompatibility and intracellular uptake. Biomaterials 29, 1807–1816.

Cohen, G.M., 1997. Caspases: the executioners of apoptosis. Biochem. J. 1, 326.

Cohen, M.S., Stern, J.M., Vanni, A.J., Kelley, R.S., Baumgart, E., Field, D., Libertino, J.A., Summerhayes, I.C., 2007. *In vitro* analysis of a nanocrystalline silver-coated surgical mesh. Surg. Infect. 8, 397–403.

Curtin, J.F., Donovan, M., Cotter, T.G., 2002. Regulation and measurement of oxidative stress in apoptosis. J. Immunol. Methods 265, 49–72.
Davila, J.C., Acosta, D., 1993. Preparation of primary monolayer of postnatal rat liver cells for hepatotoxicity assessment of xenobiotics. In: Tyson, CA, Frazier, JM (Eds.), In Vitro Biological Systems, 1. Academic, San Diego, pp. 244–261.
Fadeel, B., Ahlin, A., Henter, J.I., Orrenius, S., Hampton, M.B., 1998. Involvement of caspases in neutrophil apoptosis: regulation by reactive oxygen species. Blood 92, 4808.
Foley, S., Crowley, C., Smaihi, M., Bonfils, C., Erlanger, B.F., Seta, P., 2002. Cellular localisation of a water-soluble fullerene derivative. Biochem. Biophys. Res. Commun. 294, 116–119.
Gerlier, D., Thomasset, N., 1986. Use of MTT colorimetric assay to measure cell activation. J. Immunol. Methods 94, 57–63.
Gopinath, P., Gogoi, S.K., Chattopadhyay, A., Ghosh, S.S., 2008. Implications of silver nanoparticle induced cell apoptosis for *in vitro* gene therapy. Nanotechnology 19, 1–10.
Hanks, T.I., 1996. In vitro models of biocompatibility: a review. Dent. Mater. 12, 186–193.
Harbell, J.W., Koontz, S.W., Lewis, R.W., Lovell, D., Acosta, D., 1997. Cell cytotoxicity assays. Food Chem. Toxicol. 35, 79–126.
Hunt, T.K., Hopt, H.W., 1997. Wound healing and infection, what surgeons and anesthesiologist can do? Surg. Clin. North Am. 77, 587–606.
Hussain, S.M., Hess, K.L., Gearhart, J.M., Geiss, K.T., Schlager, J.J., 2005. *In vitro* toxicity of nanoparticles in BRL 3A rat liver cells. Toxicol. *in vitro* 19, 975–983.
Hussain, S.M., Javorina, A.K., Schrand, A.M., Duhart, H.M., Ali, S.F., Schlager, J.J., 2006. The interaction of manganese nanoparticles with PC-12 cells induces dopamine depletion. Toxicol. Sci. 92, 456–463.
Jain, P., Pradeep, T., 2005. Potential of silver-nanoparticle-coated polyurethane foam as an antibacterial water filter. Biotechnol. Bioeng. 90, 59–63.
Kono, Y., 1978. Generation of superoxide radical during auto-oxidation of dyhydroxylamine and an assay for superoxide dismutase. Arch. Biochem. Biophy. 186, 189–195.
Lee, H.Y., Park, H.K., Lee, Y.M., Kim, K., Park, S.B., 2007. A practical procedure for producing silver nanocoated fabric and its antibacterial evaluation for biomedical applications. Chem. Commun. (Camb.) 28, 2959–2961.
Li, N., Sioutas, C., Cho, A., Schmitz, D., Misra, C., Sempf, J., 2003. Ultrafine particulate pollutants induce oxidative stress and mitochondrial damage. Environ. Health Perspect. 111, 455–460.
Lopotko, D.O., Lukianova-Hleb, E.Y., Oraevsky, A.O., 2007. Clusterization of nanoparticles during their interaction with living cells. Nanomedicine 2, 241–253.
Moller, W., Hofer, T., Ziesenis, A., Karg, E., Heyder, J., 2002. Ultrafine particles cause cytoskeletal dysfunctions in macrophages. Toxicol. Appl. Pharmacol. 182, 197–207.
Morgan, K., 2005. In: Costa, G., Hodgson, L.G., Lawrence, E., Ozolins, D.A., Reed, T.R., Greenlee, D.J., Sassa, W.F., Sipes, S. (Eds.), Current Protocols in Toxicology. John Wiley & Sons.
Renvoize, C., Biola, A., Pallardy, M., Breard, J., 1998. Apoptosis: identification of dying cells. Cell Biol. Toxicol. 14, 111–120.
Reynolds, E.S., 1963. The use of lead citrate at high pH as an electron-opaue stain in electron microscopy. J. Cell Biol. 17, 208–212.
Saldak, J., Lindsay, R.H., 1968. Estimation of total, protein bound and non-protein sulfhydryl groups in tissue with Ellman's reagent. Anal. Biochem. 25, 192–205.
Straughan, D.W., Fentem, J.H., Balls, M., 1997. Replacement alternative and complementary *in vitro* methods in pharmaceutical research. In: Castell, J.V., Gomez-Lechan, M.J. (Eds.), *In vitro* methods in pharmaceutical research. Academic Press, California, pp. 1–13.
Takenaka, S., Karg, E., Roth, C., Schulz, H., Ziesenis, A., Heinzmann, U., Schramel, P., Heyder, J., 2001. Pulmonary and systemic distribution of inhaled ultrafine silver particles in rats. Environ. Health Perspect. 4 (Suppl.), 547–551.
Tian, J., Wong, K.K.Y., Ho, C.M., Lok, C.N., Yu, W.Y., Che, C.M., Chiu, J.F., Paul, K.H.T., 2007. Topical delivery of silver nanoparticles promotes wound healing. Chem. Med. Chem. 2, 129–136.
Trop, M., Novak, M., Rodl, S., Hellbom, B., Kroell, W., Goessler, W., 2006. Silver coated dressing Acticoat caused raised liver enzymes and argyria-like symptoms in burn patient. J. Trauma 60, 648–652.
Zhang, Y., Sun, J., 2007. A Study on the bio-safety for nano-silver as anti-bacterial materials. Chin. J. Med. Instrum. 31, 35–38.
Zhang, Z., Yang, M., Huang, M., Hu, Y., Xie, J., 2007. Study on germicidal efficacy and toxicity of compound disinfectant gel of nanometer silver and chlorhexidine acelate. Chin. J. Health Lab. Technol. 17, 1403–1406.
Zurlo, J., Arterburn, L.M., 1996. Characterization of a primary hepatocyte culture system for toxicological studies. *In Vitro* Cell. Dev. Biol. 32, 211–220.